ISIJ International, Vol. 60 (2020), No. 1, pp. 51–57

Structure and Viscosity of $CaO–Al_2O_3–B_2O_3$ Based Mould Fluxes with Varying CaO/Al_2O_3 Mass Ratios

Jiangling LI,[1,2)]* Kuochih CHOU[2)] and Qifeng SHU[2,3)]

1) College of Materials Science and Engineering, Chongqing University, Chongqing, 400044 China.
2) School of Metallurgical and Ecological Engineering, University of Science and Technology Beijing, Beijing, 100083 China.
3) Process Metallurgy Research Unit, University of Oulu, Oulu, FI-90014 Finland.

(*Received on April 14, 2019; accepted on July 16, 2019*)

The effect of CaO/Al_2O_3 ratio on the structure of $CaO–Al_2O_3–B_2O_3$ based glassy mould fluxes was investigated by employing ^{27}Al and ^{11}B Triple Quantum Magic-angle spinning nuclear magnetic resonance (3QMAS-NMR) and Raman spectroscopy. ^{27}Al and ^{11}B 3QMAS-NMR spectrums showed that Al^{3+} mainly forms $[AlO_4]$ as a network former and B^{3+} mainly forms $[BO_3]$ groups in $CaO–Al_2O_3–B_2O_3$ based glasses. Raman spectrum showed existences of different $[AlO_4]$ structure units and BO_3 pyro-borate units. In addition, deconvolution results on Raman spectrums indicate that the degree of polymerization of aluminate network in $CaO–Al_2O_3–B_2O_3$ based glasses decreases with the increase of CaO/Al_2O_3 ratio. The effect of CaO/Al_2O_3 ratio on viscosity of $CaO–Al_2O_3–B_2O_3$ based glassy mould fluxes was investigated by employing the rotating-cylinder method. The viscosity decreases with increasing CaO/Al_2O_3 ratio in $CaO–Al_2O_3–B_2O_3$ based mould flux. Correlation between viscosity and structural information of investigated mould fluxes was explored.

KEY WORDS: structure; viscosity; 3QMAS-NMR; Raman spectroscopy; $CaO–Al_2O_3–B_2O_3$ based mould flux.

1. Introduction

Recently, high Al steel (*e.g.* high Al-TRIP and TWIP steel) has received increasing attention as it has the perfect combination of strength to weight ratio and excellent ductility.[1)] Significant amounts of aluminum are added into high Al-TRIP and TWIP steel to improve properties of steel.[2)] However, high levels of Al in the steel may cause great process control problems during the continuous casting, it is due to the chemical reactions between SiO_2 in mould flux and [Al] in steel. This reaction can be illustrated by following equation:[3,4)]

$$4[Al] + 3SiO_2 = 2Al_2O_3 + 3[Si] \quad \cdots\cdots\cdots\cdots (1)$$

The above reaction between the mould flux and steel will lead to a gradual increase of alumina content and decrease of silica content in the mould fluxes. The dynamically changing of chemistry for the mould flux leads to varied physicochemical properties during the casting. As a result, there will be several casting problems presented, such as increased crack frequency, non-uniform heat transfer across the mould flux, reduced lubrication, *etc.*, and poor casting performance could be expected.[4)]

$CaO–Al_2O_3$ based mould flux is proposed to solve the problem on chemical composition change of mould fluxes during high Al steel casting.[4–6)] Some researchers have suggested some additives such as BaO, MnO and TiO_2 to adjust the properties of mould fluxes to meet the demand for casting of high Al steel.[5–7)] However, there are many problems need to be solved for application of $CaO–Al_2O_3$ based mould flux, *e.g.* strong crystallization and poor lubrication between steel shell and mould.[4,8)] The study on physiochemical properties of the $CaO–Al_2O_3$ based system is still limited to meet the demand for development of optimal mould fluxes for casting high Al steel.

In our previous work, properties of a new type of mould flux based on $CaO–Al_2O_3–B_2O_3$ system were investigated.[9)] The viscosity at 1 300°C, melting characteristics, and crystallization temperature was measured to compare with traditional mould fluxes. However, the viscosity at different temperature and structure of mould fluxes were not reported. In order to evaluate the influence of CaO/Al_2O_3 ratio on the viscosity and structure of $CaO–Al_2O_3–B_2O_3$ based mould flux, measurements on viscosity and structure of mould fluxes were carried out. The viscosity values of $CaO–Al_2O_3–B_2O_3$ based mould fluxes were measured by using the rotating spindle method. The water-quenched glassy mould fluxes subjected to Raman spectroscopy and triple quantum Magic Angle Spinning Nuclear Magnetic Resonance (3QMAS-NMR) in order to analyze the structural of glassy mould fluxes. ^{27}Al and ^{11}B 3QMAS-NMR were applied to study the local environment of Al and B in the $CaO–Al_2O_3–B_2O_3$ based glasses. All approaches provide a better knowledge of the structure of the $CaO–Al_2O_3–B_2O_3$ based glasses that should improve the understanding of the physicochemical properties of the $CaO–Al_2O_3–B_2O_3$ based melts. A correlation between viscosity and structure of

* Corresponding author: E-mail: lijiangling@cqu.edu.cn
DOI: https://doi.org/10.2355/isijinternational.ISIJINT-2019-234

mould fluxes would be established.

2. Experimental

2.1. Sample Preparation

Analytical grade $CaCO_3$, Na_2CO_3, Li_2CO_3, Al_2O_3, SiO_2 and H_3BO_3 (all purity > 99.5%) were taken as raw materials, with the $CaCO_3$ being substituted for CaO. $CaCO_3$ were calcined at 1 323 K to obtain CaO in a muffle furnace for 10 hours. Na_2CO_3, Li_2CO_3, SiO_2 and Al_2O_3 powders were also calcined at 873 K to remove moisture. After carefully weighed, the powder mixtures were ground in a mortar, about 140 g fluxes for each sample was prepared for the viscosity measurement and about 7 g fluxes for each sample were subject to the Raman and NMR measurement.

2.2. Structure Analysis

All samples were heated in a Pt crucible at 1 723 K for 3 h to ensure homogeneous melting. High temperature melts were quenched into water to form the glasses. After quenching, the samples were subject to Electron Probe Micro-Analyzer (EPMA, JEOL JXA-8230, Japan) to determine the composition. Nominal Compositions of samples and analyzed compositions of samples after melting by EPMA are listed in **Table 1**. The water-quenched samples were subjected to XRD measurements as shown in **Fig. 1**. It was confirmed that all samples are in glassy state. Glassy samples subjected to non-polarized Raman spectroscopy and Nuclear Magnetic Resonance Spectrum (NMR) measurements to determine the structure of fluxes.

Raman spectra were recorded at room temperature in the frequency range of 20–1 650 cm^{-1} using a laser confocal micro-Raman spectrometer (Horiba, LabRAM HR Evolution). The experiments were performed in room temperature using He–Cd laser with an excitation wavelength of 532 nm. All spectra were recorded between 20 and 1 650 cm^{-1}. Finally, the spectra were deconvolved using Peakfit software. During the curve-fitting procedure, widths and intensities are independent and unconstrained variables. Raman spectra were fitted by assuming Gaussian line shapes for peaks of different structural units.

The Triple Quantum Magic Angle Spinning Nuclear Magnetic Resonance (3QMAS-NMR) spectrums have been acquired using the Bruker BioSpin GmbH (400 MHz). ^{11}B 3QMAS and ^{27}Al MQMAS were used to obtained the structure information of B and Al. ^{11}B and ^{27}Al isotropic chemical shifts δiso are externally referenced relative to $BF_3 \cdot Et_2O$ and a 1 M aqueous $Al(NO_3)_3$ solution, respectively. ^{11}B and ^{27}Al 3QMAS experiments were conducted at a spinning frequency of 15 kHz. A 3-pulse z-filter sequence[10] was employed for the ^{11}B 3QMAS-NMR and ^{27}Al 3QMAS-NMR measurements. The duration of the first, second and third pulse was set to 3,1 and 11.6 μs, respectively.

2.3. Viscosity Measurements

Viscosity measurements were carried out using a rotating cylinder method with a rotary viscometer (model: RTW-10). The details about the apparatus, Mo crucible and spindle have been described in our previous works.[11] Before measurements, the viscometer was calibrated at room temperature by using standard castor oil with known viscosity. After carefully weighed, the powder mixture was ground in a mortar, about 140 g slag for each sample was subject to the viscosity measurement which was carried out in a molybdenum crucible and a graphite crucible was used to protect the molybdenum crucible on the outside of the molybdenum crucible. Firstly, the samples were held in the furnace at 1 673 K for 30 min to be pre-melted, and then quenched in air. During the procedure of viscosity measurement, all samples were held at 1 673 K for 30 min to ensure that slags were completely melted and homogeneous. Subsequently, the molybdenum spindle with a size was immersed in the molten slag and rotated at 200 r/min. After stability of the measurement, the furnace was cooled at a rate of 5 K/min and the measurement of viscosity started. Argon was used by 50 ml/min as the protective gas during the whole

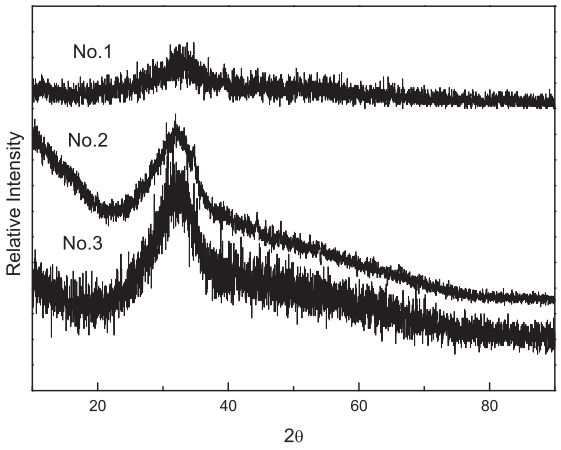

Fig. 1. XRD patterns of glassy mould fluxes.

Table 1. Chemical composition of $CaO–Al_2O_3–B_2O_3$ based mould fluxes.

Sample No.	CaO/Al_2O_3		Composition (mass%/mol%)					
			CaO	Al_2O_3	B_2O_3	Na_2O	Li_2O	T_b (°C)
1	0.9	Nominal	36/41.6	40/25.4	8/7.4	8/8.4	8/17.3	1 240
		Analyzed	36.0/41.5	38.1/24.1	9.2/8.5	8.3/8.6	8/17.2	
2	1	Nominal	38/43.5	38/24.1	8/7.3	8/8.3	8/17.1	1 211
		Analyzed	36.9/43.4	35.4/22.8	8.8/8.3	7.5/8.0	8/17.6	
3	1.11	Nominal	40/45.3	36/22.4	8/7.2	8/8.2	8/16.9	1 155
		Analyzed	40.1/46.5	33.2/21.1	7.7/7.1	7.6/8.0	8/17.3	

experimental process.

3. Results and Discussions

3.1. Effect of the CaO/Al_2O_3 Mass Ratio on Structure of Glassy Mould Fluxes

Figures 2, **3** showed ^{27}Al and ^{11}B 3QMAS spectra for glassy mould fluxes samples with CaO/Al_2O_3 = 0.9, 1 and 1.11. In ^{27}Al and ^{11}B NMR studies on glasses, resolution among various $[AlO_4]$, $[AlO_5]$, $[AlO_6]$, $[BO_3]$ and $[BO_4]$ species in conventional ^{27}Al and ^{11}B MAS spectra of such glasses is poor due to the quadrupolar broadening.[12] 3QMAS-NMR can provide much better resolutions for structural analyses. In 3QMAS-NMR spectroscopy, the evolution of multiple quantum coherence is correlated with the evolution of a single quantum coherence under the conditions of fast MAS, resulting in a separation of the isotropic chemical shifts and the quadrupolar broadening in a 2D experiment.[10,13,14] In the present work, structures of several aluminoborate glasses were explored by 3QMAS-NMR technique. For the $CaO–Al_2O_3–B_2O_3$ based glasses with differing CaO/Al_2O_3 ratios, 3QMAS-NMR experiments clearly revealed the bonding information of Al and B in different coordination.

As shown in Fig. 2, the resolution of a sole and obvious signal around 65 ppm region was observed in ^{27}Al 3QMAS spectra for CaO/Al_2O_3 = 0.9, 1 and 1.11. The 1D spectrum on top is the projection onto the isotropic dimension. The previous references revealed the presence of four-, five-, and six-fold coordinated aluminum sites with resonance shifts near 60–70, 30, and 0 ppm, respectively.[12] Based on the earlier assignments,[14,15] the signal around 65 ppm belongs to the tetrahedral coordinated species $[AlO_4]$. There is no detectable intensity at $[AlO_5]$ and $[AlO_6]$ groups at the corresponding positions in spectrums of the investigated glasses. From 1D projection of ^{27}Al 3QMAS spectra for CaO/Al_2O_3 = 0.8, 1, 1.11 in Fig. 3, it can be seen that the spectrum has a

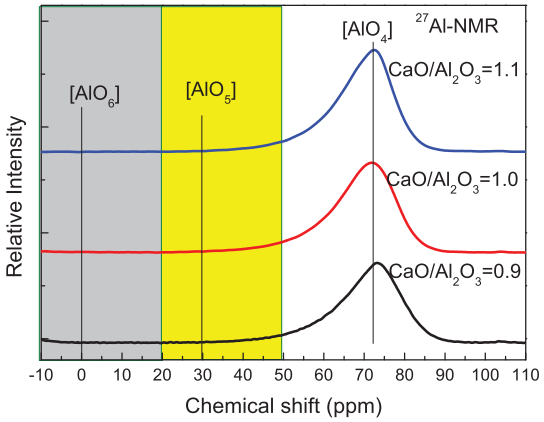

Fig. 3. 1D projections of ^{27}Al 3QMAS-NMR spectra for CaO/Al_2O_3 = 0.9, 1, 1.11. (Online version in color.)

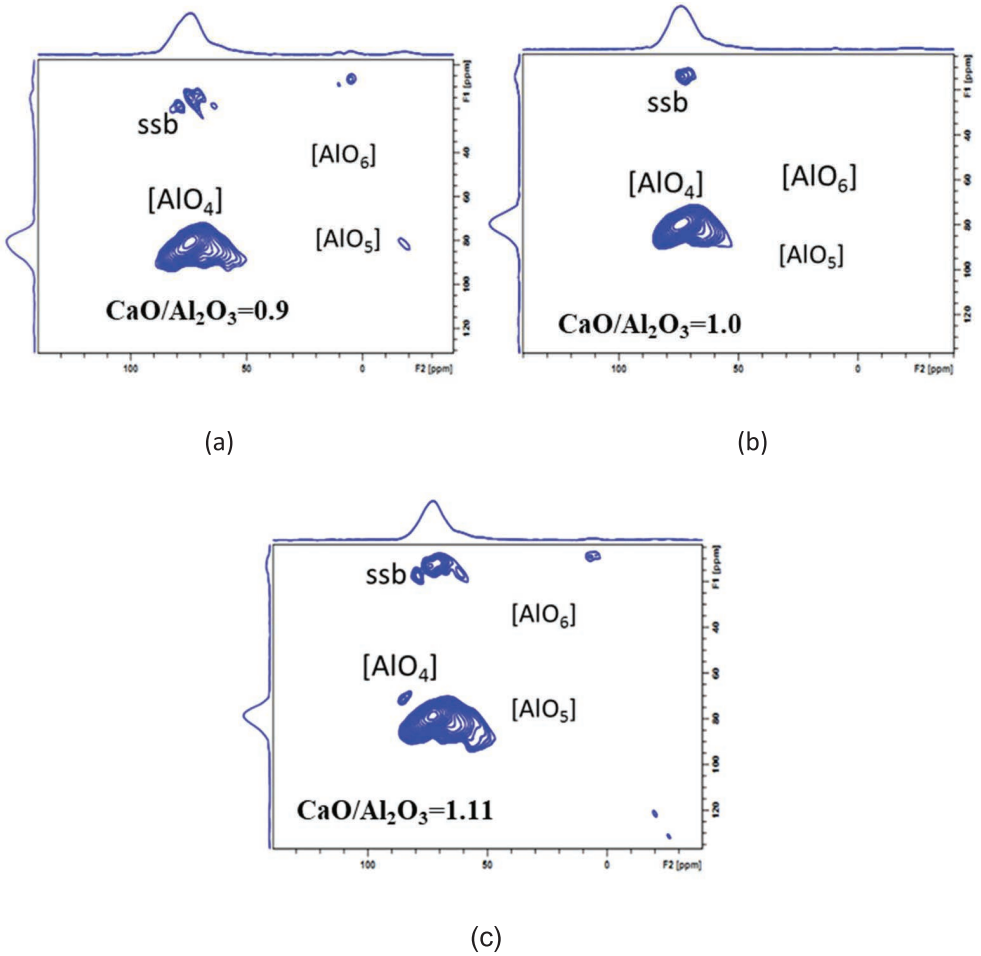

Fig. 2. ^{27}Al 3QMAS-NMR spectra for CaO/Al_2O_3 = 0.9, 1, 1.11. The peak assignable to $[AlO_4]$ sites is labeled. The low-intensity feature to the top of the main peak is a spinning sideband (SSB). (Online version in color.)

strong and broad peak centered at about 70 ppm, which is in close proximity to the chemical shift of [AlO_4]. Therefore, most of Al is exclusively connected by four oxygen of the structure in present glassy slags. It was reported that [AlO_4] is the main bond of Al in the investigated aluminoborate glasses.[13,16,17] The molar ratio of CaO/Al_2O_3 calculated from chemical compositions of mould fluxes is increased from 1.64 to 2.02 in present glassy slags. The molar ratio of CaO/Al_2O_3 is much larger than 1 which guarantees that Al^{3+} can be compensated completely to form [AlO_4] groups. Therefore, it can be concluded that Al^{3+} is mainly to form [AlO_4] as a network former. McMillan *et al.*, investigated the structure of $CaO–Al_2O_3$ glasses by ^{27}Al MAS-NMR, showed that Al formed fourfold (tetrahedral) coordination to oxygen in the glass (CaO: $Al_2O_3 \geq 1$).[18] Neuville *et al.*,[19] investigated the Al coordination and speciation in calcium aluminosilicate glasses by ^{27}Al MQ-MAS NMR, found that only AlO_4 tetrahedra are detected in calcium aluminate with low silica and high CaO content. Licheron *et al.*,[20] reported that only a characteristic of the tetrahedrally-coordinated aluminum was identified in $CaO–Al_2O_3$ glasses with $CaO/Al_2O_3 > 1$. These results are consistent with our results.

^{11}B 3QMAS-NMR spectrums for the samples with increasing CaO/Al_2O_3 ratio were shown in **Fig. 4**. [BO_3]-ring groups and [BO_3]-nonring groups at 12 ppm and 6 ppm can be discriminated by ^{11}B 3QMAS-NMR spectrums.[21] No site of [BO_4] group around 0 ppm can be found in ^{11}B 3QMAS-NMR spectrums. This indicated that almost all B^{3+} is to form [BO_3] group.

According to previous studies,[22] within a boron-containing glass, B^{3+} may be coordinated by four oxygen atoms ([BO_4] groups), or coordinated by three oxygen atoms ([BO_3] groups).Three coordinated boron may also have NBOs (asymmetric BO_3 groups). Unlike in silicates, when modifiers oxides are initially added to B_2O_3, most, if not all, [BO_3] is converted to [BO_4] without the formation of NBO. Since an increase in modifier species could introduce NBO into the system, this change has been hypothesized by the structural reaction:[22]

$$[BO_3] + NBO \Leftrightarrow [BO_4] \quad \text{..... (2)}$$

At low contents of modifier oxides in boron-rich glasses, this reaction is nearly complete.[23–25] If more modifiers are added, four coordinated boron begin to convert to asymmetric BO_3 groups. However, both the beginning point and the rate of this process depend strongly on the composition.[22] In boroaluminate glass, at high modifier contents, [BO_4] transforms into [BO_3] in part to avoid formation of $^{[4]}B–O–^{[4]}B$ and $^{[4]}B–O–^{[4]}Al$ species, which is relatively energetically unfavorable since the bridging oxygen atoms have higher net negative charges.[12,15,16] Higher modifier cation field strength favors the formation of NBO and convert [BO_4] into [BO_3].[15,26–28] In present glassy slags, the molar ratio of CaO/B_2O_3 increases from 5.62 to 6.29. It can be

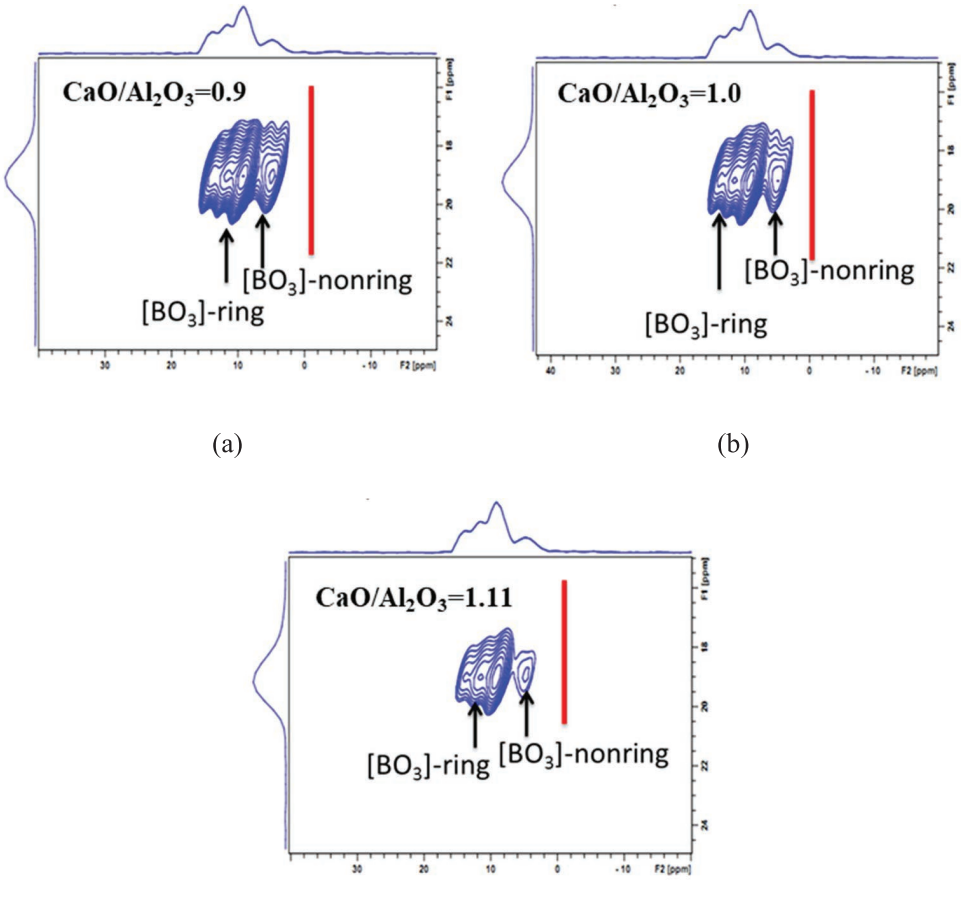

Fig. 4. ^{11}B 3QMAS-NMR spectra for CaO/Al_2O_3 = 0.9, 1, 1.11. The peak assignable to [BO_3] sites is labeled. (Online version in color.)

seen that CaO is much higher amount than B_2O_3. Due to this phenomenon, $[BO_3]$ is conclusively formed in present slags. Alkali metals and alkaline earths play dual structural roles in alkali and alkaline earth boroaluminate glass. One of these roles is to serve as network-modifiers to decrease the network degree of polymerization. In this sense, these cations are linked to terminal oxygens on tetrahedra. The other role is to charge compensate cations such as tetrahedral B^{3+} and Al^{3+}. Hayek *et al.*,[29] investigated the structure of lime alumino-borate glasses by ^{11}B NMR and ^{27}Al NMR spectroscopies and found that B^{3+} and Al^{3+} are mainly formed $[BO_3]$ and $[AlO_4]$ when the concentration of B_2O_3 is less than 8.8 mass% and the CaO/Al_2O_3 is approximately equal to 1.13. The composition of lime alumino-borate glass is very close to sample 3 in our work. This further proves the correctness of the results in our work.

In order to analyze the change of degree of polymerization of the aluminate or boroaluminate network, Raman spectrums were collected for the present glassy mould fluxes. Original Raman spectrums of all samples were shown in **Fig. 5**. It could be seen that there are three main intensity peak envelopes of the center shift at about 540 cm^{-1}, 770 cm^{-1}, 920 cm^{-1}, respectively. According to the Licheron *et al.*,[20] the Raman spectrum of C50Al50 glass consists of strong bands at 520 cm^{-1} and 790 cm^{-1}, which were identified by the transverse motions of bridged oxygens within the Al–O–Al linkages and the symmetric stretching vibration of Al–O. This is consistent to our study. These main peaks could show the information of Al–O–Al oxygen bridged bond, the network structure formed by $[AlO_4]$ and $[BO_3]$ structure. Three regions in the Raman spectra were detected: the low-frequency region (300–700 cm^{-1}), the mid-frequency region (700–900 cm^{-1}) and the high-frequency region (900–1 000 cm^{-1}). The band near 550 cm^{-1} in Al_2O_3-rich glasses is due to the presence of Al–O–Al bridges in the low-frequency region.[6,19] The bands at 770 cm^{-1} were ascribed to the Al–O stretching in differing Q^n species (n = 0.1.2.3.4, it is the number of bridging oxygen in $[AlO_4]$) in the mid-frequency region (700–900 cm^{-1}).[19,30] The Raman band at around 770 cm^{-1} shifts to lower wavenumbers with the increase of CaO/Al_2O_3 ratio. The bands at 920 cm^{-1} were attributed to the symmetric stretching vibrations of terminal oxygen atoms in orthoborate units $[BO_3]$.[19,31,32] That is to say, B^{3+} is mainly to form $[BO_3]$ groups in present slags. It is in consistence with ^{11}B 3QMAS spectra results.

The de-convoluted results of Raman spectra are showed in **Figs. 6**(a)–6(c) through the Gaussian-Deconvolution method similar to method by Mysen *et al.*[33] with the minimum correlation coefficient $r^2 \geq 0.998$. All spectrums were successfully fitted to obtain quantitative information of structure. The low-frequency region (300–700 cm^{-1}) has been fitted to two peaks in all glasses. The band near 550 cm^{-1} was due to the presence of Al–O–Al bridges. The

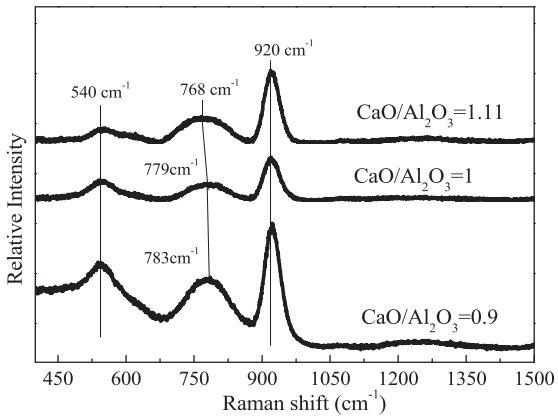

Fig. 5. Original Raman spectra for samples for CaO/Al_2O_3 = 0.9, 1, 1.11 at room temperature.

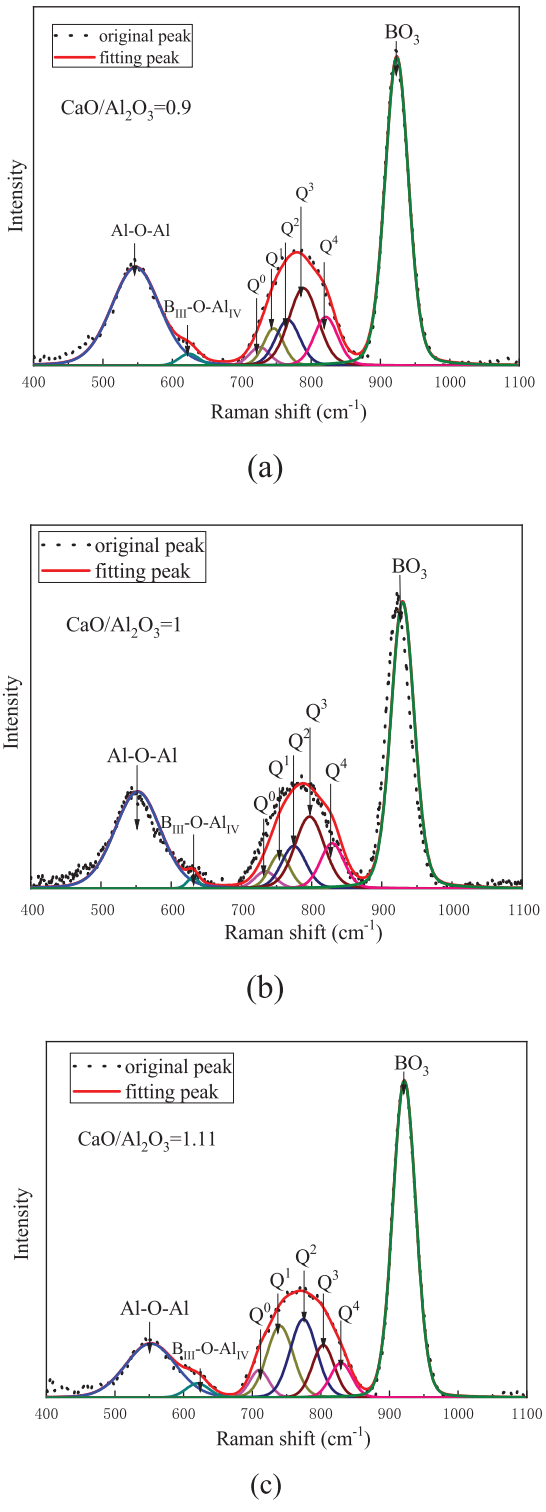

Fig. 6. The deconvoluted results of Raman spectra for CaO/Al_2O_3 = 0.9, 1, 1.11. (Online version in color.)

intensity of Raman band at around 550 cm^{-1} drastically decreased with increasing CaO/Al_2O_3 ratio. The decrease of the relative intensity of Raman band at 550 cm^{-1} indicated that the number of bridging oxygen decreased by increasing the CaO/Al_2O_3 ratio. That is to say, the aluminate structure is partly modified by the increase in the CaO/Al_2O_3 ratio. Next to the peak, the bands at 630 cm^{-1} presented a small peak, it was ascribed to B_{III}–O–Al_{IV} bending vibration.[34,35] The relative intensity of Raman band at 630 cm^{-1} had no significant changes in all glasses. Cormier *et al.*,[36,37] have reported that there have various Q^n(Al) (n = 0, 1, 2, 3, 4) species in 61 mol%CaO and 39 mol% Al_2O_3 glass. The CaO/Al_2O_3 ratio for their glass is close to that of the sample 3. Therefore, the Raman bands at 770 cm^{-1} in the mid-frequency region (700–900 cm^{-1}) has been assumed to be fitted to five kinds of Q^n structure units in present work. The Raman bands at 720 cm^{-1}, 740 cm^{-1}, 760 cm^{-1}, 780 cm^{-1} and 830 cm^{-1} correspond to the Al–O stretching vibration in [AlO_4] tetrahedral units with the NBO/Al = 4 (Q^0_{Al}), NBO/Al = 3 (Q^1_{Al}), NBO/Al = 2 (Q^2_{Al}), NBO/Al = 1 (Q^3_{Al}) and NBO/Al = 0 (Q^4_{Al}), based on the assignments of Raman bands in spectral of aluminate glass.[30,38,39] The deconvolution results were shown in **Table 2**. As seen in Table 2, Q^2_{Al} replaces Q^3_{Al} to become the strongest band with the increase of CaO/Al_2O_3 ratio. The intensity of Q^3_{Al} and Q^4_{Al} were decreased, while the intensity of Q^0_{Al}, Q^1_{Al} and Q^2_{Al} were increased with increasing CaO/Al_2O_3 ratio.

According to Frantz and Mysen,[40] the mole fractions of different structure units are related to the band areas in Raman spectra. In this work, the average number of bridging oxygen of each sample is used to explain the change of the aluminates structure network, which could be estimated by summation of the area ratio of all structural units (Q^0, Q^1, Q^2, Q^3 and Q^4) multiplied by the number of its bridging oxygen. The effects of CaO/Al_2O_3 ratio on the estimated average number bridging oxygen were shown in **Fig. 7**. It can be seen that the average number of bridging oxygen just decreased from 2.54 to 1.81 as the CaO/Al_2O_3 ratio in mass increases from 0.9 to 1.11, indicating degree of polymerization of aluminate network is decreased. Meanwhile, the NBO/T (the ratio of Non-bridging Oxygen/Oxygen in Tetragonal bonding) values have been estimated using a mathematical model reported by Mills *et al.*,[41] It was obtained that the values of NBO/T for slags with CaO/Al_2O_3 ratio of 0.9, 1.0 and 1.1 are approximately equal to 1.05, 1.19 and 1.37 respectively. The values of BO/T for slags with CaO/Al_2O_3 ratio of 0.9, 1.0 and 1.1 can be deduced to be 2.95, 2.81 and 2.63 respectively, which are shown in Fig. 7. It can be seen that the values between the Raman calculation and the mathematical model are close to each other, indicating that the estimation method for the average number of bridging oxygen in present work is reliable.

Table 2. Deconvolved results of Raman spectra for $CaO–Al_2O_3–B_2O_3$ based glasses.

Sample No.	CaO/Al_2O_3	Percentage of each unit (%)				
		Q^0_{Al}	Q^1_{Al}	Q^2_{Al}	Q^3_{Al}	Q^4_{Al}
1	0.9	6.83	13.22	19.60	39.92	20.43
2	1	7.47	14.36	30.77	32.66	14.75
3	1.11	7.75	28.15	44.26	15.52	4.32

3.2. Effects of the CaO/Al_2O_3 Mass Ratio on Viscosity

As can be seen from the viscosity curves of the mould fluxes with the w(CaO/Al_2O_3) ratio decreased from 0.8 to 1.11 in **Fig. 8**, the viscosity of $CaO–Al_2O_3–B_2O_3$ based mould fluxes decreased with the CaO/Al_2O_3 ratio increasing from 0.9 to 1.11 at the same temperature. Additionally, it can be found that with the increase of temperature, the measured viscosity decreased because of a weaker interaction among flow units caused by temperature increase. Below a critical temperature, the viscosity of mould fluxes rapidly increases with decreasing temperature. This critical temperature could be defined as a breaking temperature for mould fluxes. It can be seen from the Fig. 8 that, the breaking temperature for mould fluxes decreases with increasing CaO/Al_2O_3 ratio. The breaking temperatures from viscosity curves are mainly dependent on the thermodynamic liquidus temperature and crystallization behavior of slag. The thermodynamic liquidus temperature for slag cannot be calculated from thermodynamic package due to the limiting thermodynamic data for this new slag system. But according

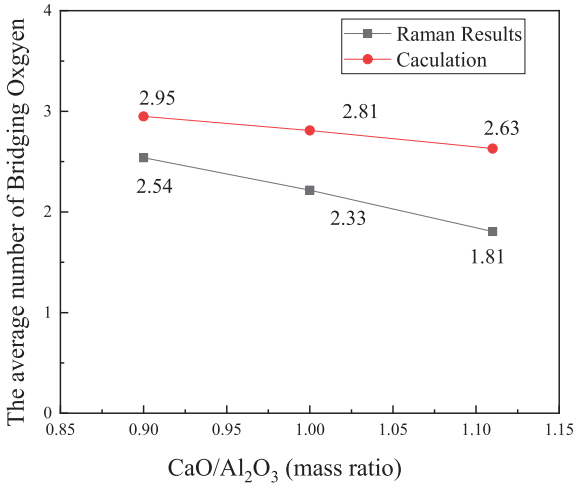

Fig. 7. The change of the average number of bridging oxgyen for CaO/Al_2O_3 = 0.9, 1, 1.11. (Online version in color.)

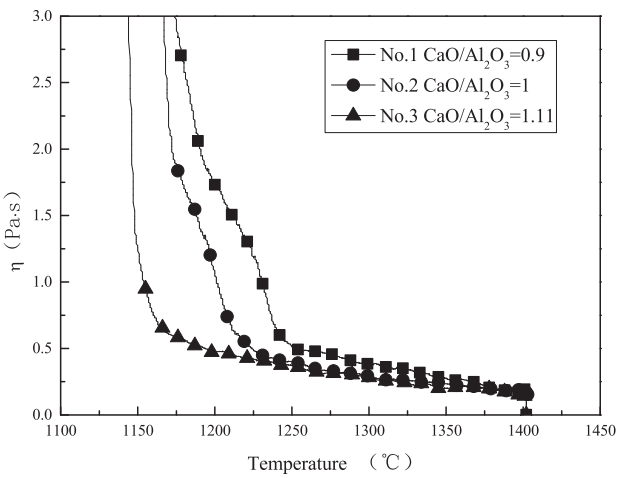

Fig. 8. Viscosity of mould fluxes with varying CaO/Al_2O_3 mass ratio as functions of temperature.

to our previous study on crystallization of the same slag,[42] the slag with the lowest CaO/Al_2O_3 ratio ($CaO/Al_2O_3 = 0.9$) has the fastest crystallization, which could also contribute to the highest breaking temperature.

Correlation between structural information and physiochemical properties of slags could be explored. Many researchers have reported that viscosity of slags has closely relationship with structure.[6,34,43,44] In this work, with the increase of CaO/Al_2O_3 ratio, more excess free oxygen ions (O^{2-}) supplied from the dissociation of CaO would lead to a gradual decrease of the bridging oxygen structure (BO) in aluminate structure and an increase of the non-bridging oxygen (NBO) in aluminate structure. This would promote the de-polymerization of aluminate structure, leading to smaller and simpler aluminate structure units. On the other hand, with increasing the CaO/Al_2O_3 ratio, more excess free oxygen ions (O^{2-}) supplied from the dissociation of CaO were introduced into borate structural units to create more NBO for borates. This also leads to the formation of many small and simple structure units of borate which is beneficial to viscous flow of slags. The modified network structures of boroaluminates have comparably smaller unit network structures resulting in lower resistance for shearing the liquid layers to decrease the viscosity. The 3QMAS-NMR and Raman spectral study in section 3.1 confirmed that the degree of polymerization of aluminates is decreased with the increase of CaO/Al_2O_3 ratio. Due to above reasons, with the increase of CaO/Al_2O_3 ratio, the viscosity of mould fluxes are decreased.

4. Conclusions

The effect of CaO/Al_2O_3 ratio on viscosity and structure of $CaO–Al_2O_3–B_2O_3$ based mould fluxes were investigated by employing the rotating-cylinder viscosity measurement in conjunction with ^{27}Al 3QMAS-NMR, ^{11}B 3QMAS-NMR and Raman spectroscopy measurements. Furthermore, the relationship between viscosity and structure has been explored. The following conclusions have been obtained.

(1) ^{27}Al 3QNMR and ^{11}B 3QNMR investigation results have shown that Aluminum mainly forms $[AlO_4]$ as a network former and Boron mainly forms $[BO_3]$ groups in $CaO–Al_2O_3–B_2O_3$ based glasses.

(2) Raman spectral investigation confirmed that boron mainly forms pyroborate (BO_3) structural units in $CaO–Al_2O_3–B_2O_3$ based glasses. In addition, deconvolution results on Raman spectral showed the degree of polymerization of aluminate network in $CaO–Al_2O_3–B_2O_3$ based glasses decreased with the increase of CaO/Al_2O_3 ratio.

(3) The viscosity of $CaO–Al_2O_3–B_2O_3$ based mould fluxes decreased as increasing CaO/Al_2O_3 ratio in $CaO–Al_2O_3–B_2O_3$ based mould fluxes. Correlation between viscosity and structural of mould fluxes could be obtained.

Acknowledgements

Financial support from the Natural Science Foundation of China (NSFC contract No. 51774026 and 51704050) and the Academy of Finland for Genome of steel grant (No. 311934) is gratefully acknowledged.

REFERENCES

1) A. Grajcar, R. Kuziak and W. Zalecki: *Arch. Civ. Mech. Eng.*, **12** (2012), 334.
2) O. Grässel, L. Krüger, G. Frommeyer and L. W. Meyer: *Int. J. Plast.*, **16** (2000), 1391.
3) M. S. Kim, S. W. Lee, J. W. Cho, M. S. Park, H. G. Lee and Y. B. Kang: *Metall. Mater. Trans. B*, **44** (2013), 299.
4) J. Cho, K. Blazek, M. Frazee, H. Yin, J. H. Park and S. Moon: *ISIJ Int.*, **53** (2013), 62.
5) D. Xiao, W. Wang and B. Lu: *Metall. Mater. Trans. B*, **46** (2015), 873.
6) J. L. Li, Q. F. Shu and K. C. Chou: *Can. Metall. Q.*, **54** (2015), 85.
7) H. Zhao, W. Wang, L. Zhou, B. Lu and Y. Kang: *Metall. Mater. Trans. B*, **45** (2014), 1510.
8) J. Li, Q. Shu, X. Hou and K. Chou: *ISIJ Int.*, **55** (2015), 830.
9) J. Li, B. Kong, B. Galdino, J. Xu, K. Chou, Q. Liu and Q. Shu: *Steel Res. Int.*, **88** (2017), 1600485.
10) V. Lacassagne, P. Florian, V. Montouillout, C. Gervais, F. Babonneau and D. Massiot: *Magn. Reson. Chem.*, **36** (1998), 956.
11) J. L. Li, Q. F. Shu and K. Chou: *Ironmaking Steelmaking*, **42** (2015), 154.
12) B. C. Bunker, R. J. Kirkpatrick, R. K. Brow, G. L. Turner and C. Nelson: *J. Am. Ceram. Soc.*, **74** (1991), 1430.
13) K. U. Gore, A. Abraham, S. G. Hegde, R. Kumar, J. Amoureux and S. Ganapathy: *J. Phys. Chem. B*, **106** (2002), 6115.
14) J. H. Baltisberger, Z. Xu, J. F. Stebbins, S. H. Wang and A. Pines: *J. Am. Ceram. Soc.*, **118** (1996), 7209.
15) L. Du and J. F. Stebbins: *J. Non-Cryst. Solids*, **351** (2005), 3508.
16) L. Züchner, J. C. C. Chan, W. Müller-Warmuth and H. Eckert: *J. Phys. Chem. B*, **102** (1998), 4495.
17) H. Deters, A. S. de Camargo, C. N. Santos, C. R. Ferrari, A. C. Hernandes, A. Ibanez, M. T. Rinke and H. Eckert: *J. Phys. Chem. C*, **113** (2009), 16216.
18) P. F. McMillan, W. T. Petuskey, B. Coté, D. Massiot, C. Landron and J. Coutures: *J. Non-Cryst. Solids*, **195** (1996), 261.
19) D. R. Neuville, L. Cormier and D. Massiot: *Chem. Geol.*, **229** (2006), 173.
20) M. Licheron, V. Montouillout, F. Millot and D. R. Neuville: *J. Non-Cryst. Solids*, **357** (2011), 2796.
21) L. Du and J. F. Stebbins: *J. Phys. Chem. B*, **107** (2003), 10063.
22) J. Wu: Ph.D. thesis, Stanford University, (2011), 3.
23) R. J. Araujo: *J. Non-Cryst. Solids*, **58** (1983), 201.
24) B. C. Bunker, D. R. Tallant, R. J. Kirkpatrick and G. L. Turner: *Phys. Chem. Glasses*, **31** (1990), 30.
25) W. J. Dell, P. J. Bray and S. Z. Xiao: *J. Non-Cryst. Solids*, **58** (1983), 1.
26) T. J. Kiczenski, L. Du and J. Stebbins: *J. Non-Cryst. Solids*, **351** (2005), 3571.
27) S. Sen, Z. Xu and J. F. Stebbins: *J. Non-Cryst. Solids*, **226** (1998), 29.
28) J. F. Stebbins and S. E. Ellsworth: *J. Am. Ceram. Soc.*, **79** (1996), 2247.
29) R. El Hayek, F. Ferey, P. Florian, A. Pisch and D. R. Neuville: *Chem. Geol.*, **461** (2017), 75.
30) T. S. Kim and J. H. Park: *ISIJ Int.*, **54** (2014), 2031.
31) L. M. Osipova, A. A. Osipov and V. N. Bykov: *Glass Phys. Chem.*, **33** (2007), 486.
32) G. D. Chryssikos, E. I. Kamitsos and A. P. Patsis: *J. Non-Cryst. Solids*, **202** (1996), 222.
33) B. O. Mysen, L. W. Finger, D. Virgo and F. A. Seifert: *Am. Mineral.*, **67** (1982), 686.
34) G. H. Kim and I. Sohn: *Metall. Mater. Trans. B*, **45** (2014), 86.
35) I. Polyakova, V. Klyuev, B. Pevzner, V. Goncharuk, O. Yanush, T. Markova, V. Maksimov and V. Kabanov: *Phys. Chem. Glasses B*, **51** (2010), 52.
36) L. Cormier, D. Ghaleb, D. R. Neuville, J. Delaye and G. Calas: *J. Non-Cryst. Solids*, **332** (2003), 255.
37) L. Cormier, D. R. Neuville and G. Calas: *J. Am. Ceram. Soc.*, **88** (2005), 2292.
38) P. McMillan and B. Piriou: *J. Non-Cryst. Solids*, **55** (1983), 221.
39) L. Hwa, S. Hwang and L. Liu: *J. Non-Cryst. Solids*, **238** (1998), 193.
40) B. O. Mysen and J. D. Frantz: *Am. Mineral.*, **78** (1993), 699.
41) K. C. Mills, L. Yuan, Z. Li and G. Zhang: *High Temp. High Press.*, **42** (2013), 3.
42) Q. Shu, J. Klug and Q. Li: *ISIJ Int.*, **59** (2019), 1057.
43) C. Feng, J. Tang, L. Gao, Z. Liu and M. Chu: *ISIJ Int.*, **59** (2019), 31.
44) Z. J. Wang, Q. F. Shu, S. Sridhar, M. Zhang, M. Guo and Z. T. Zhang: *Metall. Mater. Trans. B*, **46** (2015), 758.